© Universiti Tun Hussein Onn Malaysia Publisher's Office

IJIE

Journal of Science and Technology

Journal homepage: http://penerbit.uthm.edu.my/ojs/index.php/jst
ISSN : 2229-8460 e-ISSN : 2600-7924

A Review of Metal Injection Moulding on WC-Co Cemented Carbide Comprised of Grain Growth Inhibitors (GGI)

Siti Nur Fatimah Khairudin[1], Hazriel Faizal Pahroraji[2*], Siti Khadijah Alias[2], Mohd Halim Irwan Ibrahim[3]

[1]Faculty of Mechanical Engineering,
Universiti Teknologi MARA, 40450 Shah Alam, Selangor, MALAYSIA

[2]Faculty of Mechanical Engineering,
Universiti Teknologi MARA Kampus Pasir Gudang, 81750 Masai, Johor, MALAYSIA

[4]Faculty of Mechanical and Manufacturing Engineering,
Universiti Tun Hussein Onn Malaysia, 86400 Parit Raja, Batu Pahat, Johor, MALAYSIA

*Corresponding author

DOI: https://doi.org/10.30880/ijie.2022.14.01.009
Received 16 April 2020; Accepted 2 November 2020; Available online 07 March 2022

Abstract: This paper aims to provide a summary of metal injection moulding technologies utilising cemented WC-Co carbides comprised of grain growth inhibitors (GGI). The advanced manufacturing of metal injection moulding (MIM) has the ability to produce cement nanostructured carbides. In addition, the nature of the feedstock plays a crucial role when manufacturing a defect-free component at each point of the MIM phase, thus the interactions between the metal powder and the binder combining, moulding, and debinding are important to be recognised. The primary objective of this analysis is to investigate the characterization of feedstock to form a homogenous mixture. There are five criteria to classify features of the feedstock which include powder characteristics, binder composition, powder content ratio, mixing cycle, and approaches to palletization. Not only that, the feedstock must meet specific criteria; higher powder loading with excellent flowability by the rheological approaches. The second goal of the research is to re-evaluate feedstock's flow properties in relation to rheological activity in terms of index flow behaviour (*n*), activation energy (E), and mouldability (α). MIM practitioners have continued to underestimate erratic product quality, including inadequate regulation, distortion, and internal and external defects. These defects can arise in the early processing phases, but often occur only after sintering or debinding. The approaches are also challenging to provide. This chapter includes a description of MIM defects. Explanations are listed and recommendations are provided for these defects.

Keywords: metal injection moulding, WC-Co, grain growth inhibitor

1. Introduction

Powder metallurgy is the manufacturing process of production and utilization of metal powder as the raw material in terms of fabricating parts of high precision and accuracy. Powder metallurgy consists of a simple method. The cycle starts with the process of powder mixing with lubricants or binders, compaction process into the desired shape, and sintering process. The end process with alternative secondary process is manufacturing and finishing to deliver the powder metallurgy product quality and precision. Metal Injection Moulding (MIM) is classified as among the technologies of powder metallurgy. MIM is commonly used for high volume production due to small parts and complex shapes. During the MIM process, the four key steps are mixing, injection moulding, debinding, and sintering. Figure 1 illustrates the flow process of metal injection moulding. Generally, feedstock mixing is done to get a

*Corresponding author: hazriel@uitm.edu.my

homogenous mixture of the binder system and metal powder. The purpose of the binder system is to get the mouldability of metal powders. The mixture should be homogenized from any segregation of materials. Then, injection moulding is the process of forming material into the desired shape, also known as green part by heating the feedstock. Thereafter, debinding is the removal of the binder from the part moulded. Once the debinding process is completed, the component is known as 'brown', and the sintering process is performed to get the final product. Subsequently, the sintering process where green compact will be heated involves the temperature. The temperature is usually about 70-90% below the melting point of the metal. The sintering process is aimed at creating the structure and relation of the particle parts. To ensure that the component is mechanically resistant, the best final intensity depends on temperature.

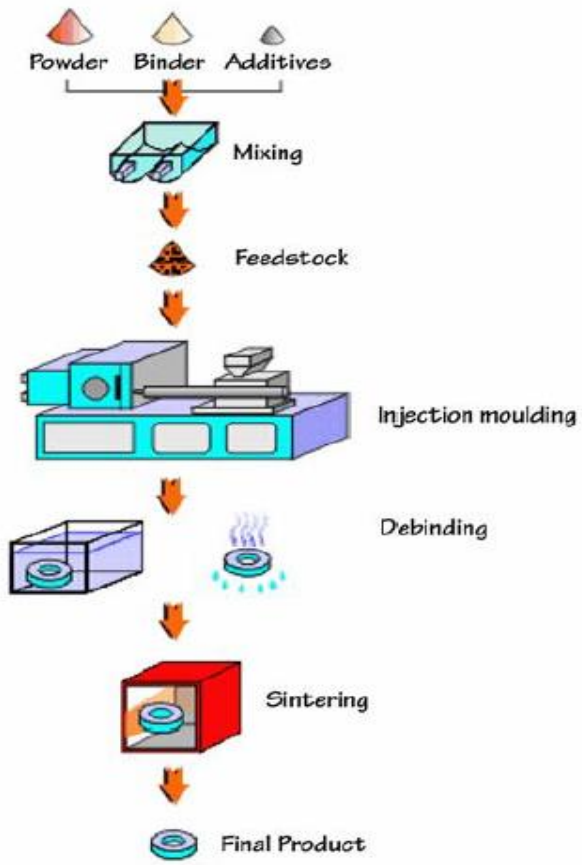

Fig. 1 - Powder injection moulding process (Karatas et al., 2004).

The first process of the MIM cycle is the preparation of feed materials. The feedstock is recognized as a powder-binding mixture. There are five criteria to classify features of the feedstock which include powder characteristics, binder composition, powder content ratio, mixing cycle, and approaches to palletization. The feedstock comprises of metal or ceramic powder and thermosetting or thermoplastic binder to ensure the required level of fluidity of the powder/binder mixture (feedstock) is achieved for effective injection moulding (Karatas et al., 2004). Homogeneity is a crucial characteristic of feedstock. Homogeneous distribution of powder particles and binders in the feedstock is vital as it aids to reduce segregation during injection moulding, and acquires isotropic shrinkage throughout the debinding and sintering techniques (Quinard et al., 2009). Next, eliminating the segregation of components of the feedstock is important to prevent too much porosity, warp, and cracking of the sintered portion (Thornagel, 2010).

The binder is a temporary weapon which helps the particles of powder to flow into the mould, and keeps the powder until the early sintering process. Binder system plays a pivotal role in determining the subsequent stage in MIM, and any failure cannot be overturned in one stage of MIM until the next stage, so that each stage requires the optimum result to be obtained and the defects to be reduced. Heterogeneous feedstock widely influences poor flow behaviour during moulding, and complicates the densification and dimensional stability of the final product. Technically, the binder should fulfil the required criteria, which are good interaction with metal powder, as it provides improved flow characteristic, able to be easily debound, environmentally safe and easy to dispose of, and comparatively low cost. The ratio of powder to binder often dictates the effectiveness of the subsequent process as well as its failure. An important feature is the composition of the binder because it also facilitates the fluidity and rigidity of the feedstock during mixing, injection, and debinding (M. Y. Anwar and H. Davies, 1995). Apart from this, there are additional requirements for the properties of binders for metal injection moulding (MIM). For example, a low viscosity

feedstock is acceptable for rapid microdetail filling during injection moulding before the feedstock consolidates (Z. Y. Liu et al., 2001). It is well recognized that high-viscosity feedstock makes moulding difficult (M. Y. Cao et al., 1991). The viscosity is persuaded by the particle size distribution, the particle form, and the powder density. To achieve an effective manufacturing process, a rheological analysis may be carried out to determine the stability of the feedstock. Rheological testing, where the rheological activity is expressed in terms of viscosity, is related to shear stress and shear intensity. This describes the feedstock properties. It is recognized that the viscosity is controlled within a small range, and the moulded component will achieve the desired shape without any physical deficiencies.

2. Material Powder: WC-Co Cemented Carbide

Since the beginning of the 20th century, cemented carbide has been extensively utilized for mining, machining, perforating, and cutting instruments, together with wear components and less chip forming tools due to its unusual high hardness, high toughness, mild elasticity, and superb wear strength to make hard metal (Prathabrao et al., 2017), (Jiang et al., 2015). Cemented carbide materials have microstructures consisting of hard carbides, with their unique properties embedded in ductile metal matrix. Generally, cemented carbides use tungsten carbide (WC), titanium carbide (TiC) or tantalum carbide (TaC) as the aggregate. The "carbide" and "tungsten carbide" usually refer to the cemented composites (Childs, 2000). Meanwhile, nanostructured cemented carbides are the most widely studied in powder metallurgy materials due to the extraordinary combination of extremely fine-grained homogeneous microstructure with good mechanical properties. Therefore, the mechanical properties depend on the microstructure developed in the sintered parts, which are regulated by combinations of factors, the crystallite size of Tungsten Carbide (WC), the binding phase free path, and WC grain contiguity (Fabijanić et al., 2014), (Al-Aqeeli et al., 2014). Tungsten carbide (WC) is classified as an alloy of outstanding toughness and wear resistance combination. The grain size is typically between 0.2 and 20 μm, and the standard carbide process proportion is between 70% and 97% of the composite weight (Pahroraji et al., 2020). The hardness and toughness of cemented carbides can be improved by reducing the WC grain to the nanoscale. Cemented carbide materials have a strong refractory carbide microstructure embedded in ductile metal materials, which give them their unique characteristics. These parameters affect the growth rate in cemented carbide, including the most commonly studied inhibitor concentrations, but no additional inhibition of grain growth over a certain concentration is achieved (Morton et al., 2005). Ideally, a variety of factors will influence the microstructure and mechanical properties of WC-Co materials during the manufacturing process particularly the form and granularity of WC-Co raw grains, WC-Co powders content, the range and quality of grain growth inhibitors, and the milling and sintering conditions (Amin et al., 2012), (Abdolali Fayyaz et al., 2014), (Jiang et al., 2015).

3. Grain Growth Inhibitors (GGI)

Chromium, tantalum carbide, and vanadium carbide are the most commonly used in the cemented carbide industry as plant growth inhibitors (GGI). GGI preference is based on the overall effectiveness, VC > Cr3C2 > NbC > TaC > TiC, which is arranged from the most effective to the least (SU et al., 2015). Each GGI has benefits and inconveniences. For example, vanadium carbide is generally more useful than chromium in preventing irregular grain growth, but the drawback is that vanadium carbide can make the commodity more fragile. Keeping the average grain size of the sintered product is one of the major problems with nano-scaling sintering powders. Due to the very high sintering behaviour of WC nanopowder, nanostructured cemented carbides are attempted to be achieved (Fabijanić et al., 2016), (Al-Aqeeli et al., 2014). A small amount of grain growth inhibitor is applied to the WC-Co to preserve the particle size of the sintered product's starting material. However, this affects the properties of the consolidated samples at the same time by decreasing the density, increasing hardness value at room temperature, and also affecting strength, hardness, and creep resistance at high temperatures (Weidow et al., 2009), (Gille et al., 2002), (Sun et al., 2008).

Also, adding TiC in WC-Co increases the hardness and wear-resistance of the WC-TiC-Co alloy, in general, better than that of the WC-Co cemented carbide, because titanium carbide is stronger and more wear resistant compared to tungsten carbide. Instead of cemented carbide, the flexural strength of cemented carbide from WC-TiC-Co decreases to a lesser degree, with lower temperature increase. The problems of work softening, short service life, and low red toughness can be remedied with cemented carbide from WC-TiC-Co (Y. Chen et al., 2018). With the incorporation of 6 to 30% titanium carbide into WC-Co, tungsten carbide could boost alloy performance in gleaming red, high hardness, and resistance to oxidation and corrosion. Homogeneous microstructure with no growth of the grain and homogenous distribution of cobalt between grains of carbide leads to optimum strength and improved toughness and hardness, whereas microstructural irregularities, such as porosity and particularly abnormal grain growth, lead to poor cross breakage strength (Mannesson, n.d.). For instance, an experiment carried out by Lee et al. (2006) investigated the implications of WC/TiC grain size ratio on microstructure and mechanical properties of WC-TiC-Co cemented carbides. When WC grain size was finer than TiC grain size, coarser TiC and (Ti, W)C phases were assigned as reinforcements in finer WC-Co matrix phase in the microstructure of WC-TiC-10 wt%Co carbides and the transverse fracture strength of WC-20TiC-10Co increased with a decrease in the WC/TiC grain size ratio (Lee et al., 2006). Besides, to enhance the physical properties of the sintered structure, tantalum carbide (TaC) is usually added to the powder attrition of tungsten carbide/cobalt (WC-Co). It also acts as grain growth inhibitor to prevent large grains from

forming, thus achieving optimal hardness (Merwe & Sacks, 2013). Siwak et al. studied on the microstructure and mechanical properties of WC−Co, WC−Co−Cr_3C_2, and WC−Co−TaC cermet fabricated via spark plasma sintering. They summarized that TaC additives enhanced the hardness and strength of fractures of the sintered compacts obtained regarding the microstructure densification and some mechanical properties (Siwak & Garbiec, 2016). Mahmoodan et al. considered TaC as an efficient inhibitor of grain growth WC-10Co during sintering, and increased the durability and strength of fracture of bulk samples. According to the result of WC-10Co, sintered samples had better effects on hardness with the addition of 0.6 %wt of TaC. The liquid phase (Co) dissolved during sintering and the WC solution was limited in phase, once TaC was introduced into the system. Therefore, the kinetic growth of WC grains decreased as a result of the addition of TaC (Mahmoodan et al., 2009).

4. Powder: Binder Ratio (Critical Powder Loading)

Critical powder loading is the composition in which the particles are packed without external pressures as tightly as possible and all space between the particles is filled with the binder. Critical powder loading in MIM depends on various factors, such as powder size, shape and distribution, binder essential feature, and feedstock combination of homogeneity. The critical powder loading affects the particle size dramatically. The smaller the size of the particle, the higher the surface region in the lower powder loading (Zakaria et al., 2014). Most feedstock is significantly less powder formulated than critical solid loading. Every particle of powder in the feedstock should be preserved by a very thin film binder. In the meantime, binders fill all space between the powder particles. The volume of critical powder loading is normally 10-20% higher than the powder tap density. Optimum loading of powder is typically 2-5% lower than critical loading. These data might be useful as fundamental ratios when working on the new rheological behaviour of feedstock [7]. Apart from that, other principles contribute to the critical packing of powder. A large excess binder is not appropriate because during the moulding process, the excess binder is removed from the powder resulting in flashing or diversity in the moulded sections. Therefore, the wide binder surplus during debinding delivers compact slumping, as the particles are not preserved after extracting the binder. Too little binding also causes high viscosity and trapped air pockets, which make moulding difficult (Subaşı et al., 2019). Higher powder loading is extremely important for the mass production of complex and responsive MIM components because of smaller compact volume shrinkage and easier tolerance regulation. However, too high loading of powder is also impractical, as it will result in very high viscosity of feedstock, resulting in failures in injection moulding (Li et al., 2007). Three potential situations arise for a powder binder mixture, as sketched in Figure 2. There is a crucial loading of the powder where the binder is enough to form a strong assimilation layer of the powder particles, and fill the voids of the inter-particles (see Figure 2(b)). This is the compressed powder particle packing. Once the powder loading is higher than the critical one, there is not enough binder to fill the space between the particles in the powder. Therefore, the feedstock contains voids (see Figure 2(a)). Furthermore, Figure 2(c) illustrates lower powder loading than the critical one because it contains so much binder. As a result, large volume shrinkage after the debinding and sintering process makes compact tolerance to small dimensions very complicated.

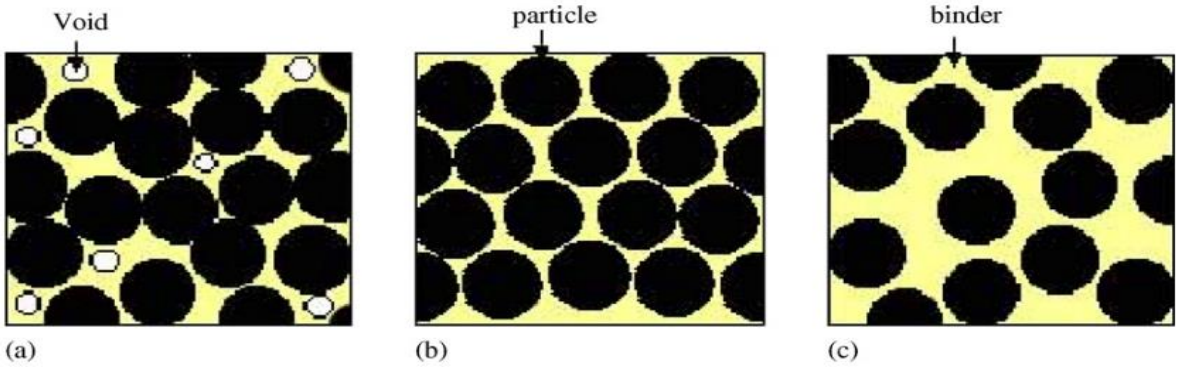

Fig. 2 - Three possible situations in a powder-binder mixture (Li et al., 2007)

4.1 Binder Composition

For the fortunate mixing of MIM compounds, the rheological properties of the binder are essential when looking for a customized formulation of the binder or selecting the correct additive. Technically, the binder should fulfil the required criteria. Table 1 summarises the essential characteristics needed for binders. These qualities are classified into commercially related types, powder interactions, flow behaviour, material properties, and debinding properties. The binder or binder system usually has three components; a low molecular weight part providing the flowability needed during moulding, a backbone polymer delivering green strength, and a surfactant functioning as a bridge of the binder of powder particles (P. Cao & Hayat, 2020). More recent works in MIM extend the method by using a binder

formulation consisting of at least more than one component. The formulation of the binder is a decisive element because it encourages the fluidity and rigidity of the feedstock, particularly during mixing, injection moulding, and debinding.

Table 1 - Attribution of an Ideal Binder (P. Cao & Hayat, 2020)

Commercially related types	• Inexpensive • Easily available • Safe and environmentally acceptable • Log shelf • Low water absorption
Powder interactions	• Excellent powder wetting (low touch angle) • Strong powder adhesion • Chemically inactive for powder • Powder particle capillary attraction • Thermally reliable within mixing and moulding process
Flow behaviour	• Low viscosity (≤10Pa.s) • Adequate strength at room temperature (≥4MPa) • Rapidly solidify in viscosity during cooling
Material properties	• Good power and rigidity • Low coefficient of thermal expansion • Strong thermal conductance • Not affected by cyclic heating
Debinding properties	• The temperature of degradation should be above moulding and temperature mixing • Progressive temperature decomposition • Products decompose non-corrosive and non-toxic • Low residual burnout char

The effective mixing and homogeneity of the feedstock depend on the adhesion to metal powder of the binder method. Thus, the binder system should have a low contact angle with metal particles. The low contact angle contributes to better attachment of powder particles that helps mixing and moulding processes. The binding mechanism and the metal powder particles are mutually inert with respect to each other. To achieve a defect-free moulding operation, the feedstock should possess certain rheological traits. Researchers must properly select the test set-up for rheological measurements. The best way to predict the flow activity of MIM compound is currently realized by a capillary rheometer. Capillary rheometer measures the fluid's viscosity by assessing the pressure required to allow the fluid to flow through a narrow cylindrical tube or rectangular slit. The feedstock viscosity should be in an optimal range. Too low viscosity may trigger problems including flashing and isolation of the binder powder during moulding. Too high viscosity can impact the mixing and moulding phase. An effective formation process depends on the flow activity of the feedstock. The feedstock should be pseudoplastic (i.e. reduced viscosity with rising shear rates), ensuring standardised filling of the cavity of the mould and the product's shape conservation. Karatas et al. explored the rheological properties of ceramic feed materials with steatite powder, using polyethylene (PE) and three waxes (carnauba, beeswax, and paraffin). The research reported that the proposed formulation fulfilled the specific requirement and was suitable for moulding by injection. The flow behaviour index (n) parameters were figured to be less than 1, as pointed by pseudoplastic behaviour. Najla et al. investigated the flow behaviour and injectability of SS17-4PH with palm stearin (PS) and polyethylene (PE) binders in powder injection moulding. They finalized the appropriateness of 60wt% PS and 40wt% PE as binders for SS17-4PH, where a pseudoplastic flow occurred from the rheological behaviour investigation due to the suitable range of viscosity and shear rate needed in PIM with the lowest value for activation energy, *E*, as the feedstock had low-temperature sensitivity and changed in pressure. The binder should preferably be simple to extract without causing defects in injection moulded components, with a reasonable pace. The green component is more vulnerable to defects during the debinding phase. Ineffective polymer backbone strength results in poor structure stability throughout the initial decomposition period. The weak interconnected open porosity of thermal debinding results in the creation of deficiencies, such as cracking and blistering.

5. Ball Mill Effects on Powder Characteristics

A ball mill is a kind of grinder used for grinding, combining, and mixing materials occasionally. This is based on impact and attrition, which is based on the energy released at the time of ball collision, as well as the high grinding energy generated by ball friction on the wall as illustrated in Figure 3. When the mill rotates, balls are picked up by the mill wall, and rotate around the wall because of the centrifugal force, which causes a frictional effect to grind the material. On the other hand, the reversed rotation of the disc also applies to the mill, where centrifugal force is applied in the opposite direction, causing the balls to turn on the opposite walls of the mill. Most of the reduction is accomplished by the impact in the ball mill.

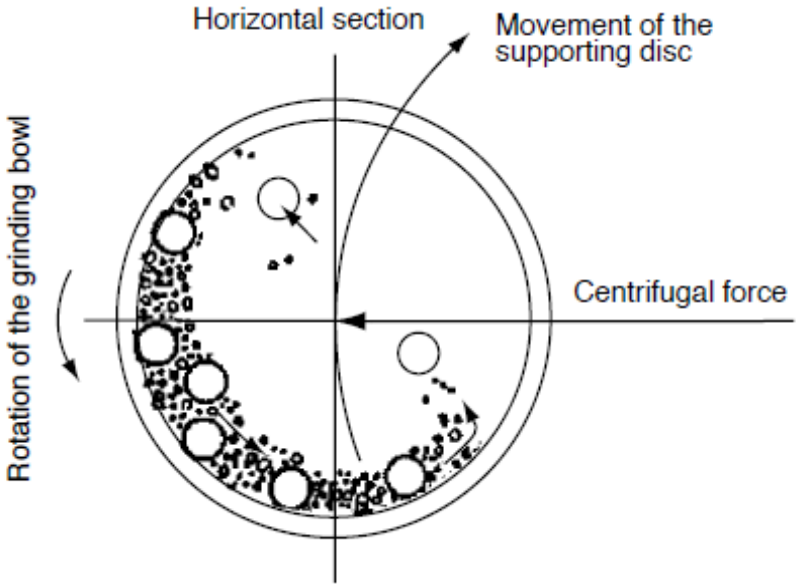

Fig. 3 - Ball milling method operating theory (Baheti et al., 2012)

Ball milling performance depends on the surface area of milling media used throughout the process. The method of milling is influenced by the amount of touch points between the balls and the particles (El-Eskandarany, 2015). The large ball provides higher energy during movement of the mill and higher energy impacts between balls and ball milling vials that may enhance particle deformation and fracture, while also improving the reduction in grain size. The medium size of the balls can help grinding particles to avoid cold welding to agglomeration. Smaller balls have less energy effects (Zhang et al., 2008). However, very big balls induce extreme agglomeration, which reduces particle size. Figure 4 demonstrates the influence of ball size on the energy emitted. It is noticeable that the additional impact energy can be passed to powder particles if the bigger milling ball is used due to increase in ball mass.

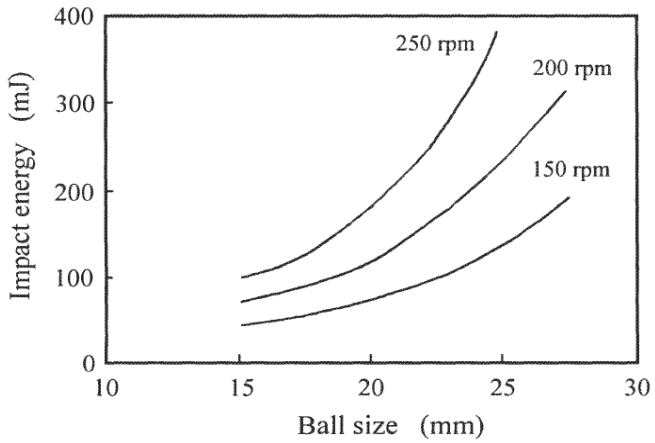

Fig. 4 - Influence of ball size on impact energy (L. Chen & Al, 2001)

A previous research has established that the formulae to determine the ball diameter depend on the diameter of the grain size material being ground (Magdalinovic et al., 2012). The general form is given in the equation below.

$$d_b = Kd^n \tag{1}$$

where d_b is the ball diameter, d is the diameter of the grain size material being ground, K and n are parameters, for which all authors say, depend on mill characteristics, grinding conditions and characteristics of the material being ground and which are consequently determined by experiments. In many cases, the grain size distribution of a ball mill feed is well described by Gaudin-Schumann's equation.

$$d^* = \left(\frac{d}{d_{max}}\right)^m \tag{2}$$

where d^* is the grain fill level less than d, d is the grain diameter, d_{max} is the maximum grain diameter, and m is the exponent which characterizes the grain size distribution. The optimal ball charge in a mill should be made up in such a way that the ball size distribution of a charge should be in accordance with Gaudin-Schumann's equation.

$$Y_E = \left(\frac{d_b}{d_{b\,max}}\right)^c, d_{bmin} < d_b < d_{b\,max} \tag{3}$$

where Y is the ball fill level having the diameter less than d_b, d_b is the ball diameter, d_{bmax} is the maximum ball diameter in the charge, $dbmin$ is the minimum ball diameter which can grind efficiently in a mill, c is the exponent which characterizes the ball size distribution so that the most efficient grinding can be achieved if the condition $m=c$ is fulfilled. Jidong et al. (2013) found that the linked carbonyl nickel chain is broken and the mixture is even and well distributed by using a ball mill (see Figure 4(b)). Hence, a smaller mean particle size and a wider range of distribution instead of the mixture without a ball mill are achieved. Figure 4(a) shows carbonyl iron and carbonyl nickel which also retain both their original morphologies, and have high agglomeration tendencies. Figure 6(a) and Figure 6(b) indicate a wider mean particle size and a broader distribution range of particle size (Ma et al., 2014). The method of ball milling results in the elimination of agglomerated powder and the improvement of dispersion. Therefore, the value distribution slope parameter diminishes significantly, which is perfect for increasing powder loading.

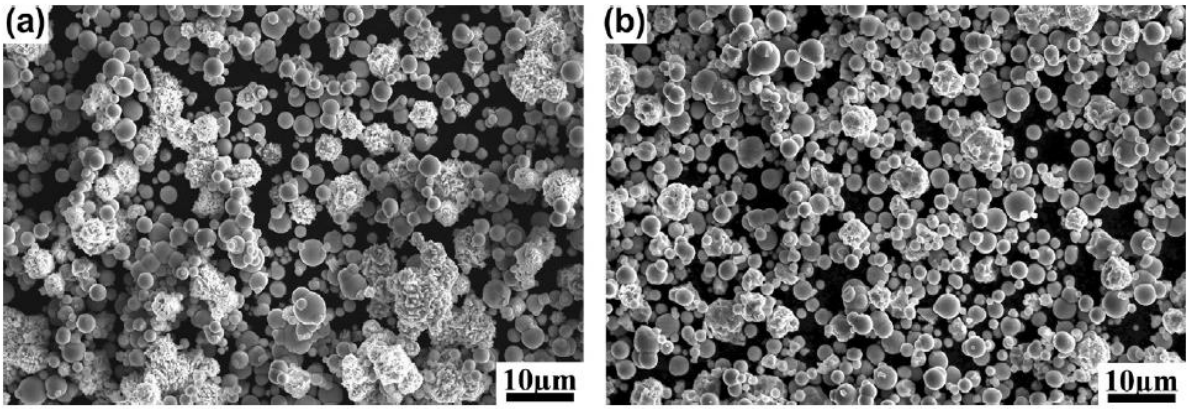

Fig. 5 - Morphology of mixed powder, (a) mixed powder without ball mill process; (b) mixed powder after ball mill process (Ma et al., 2014)

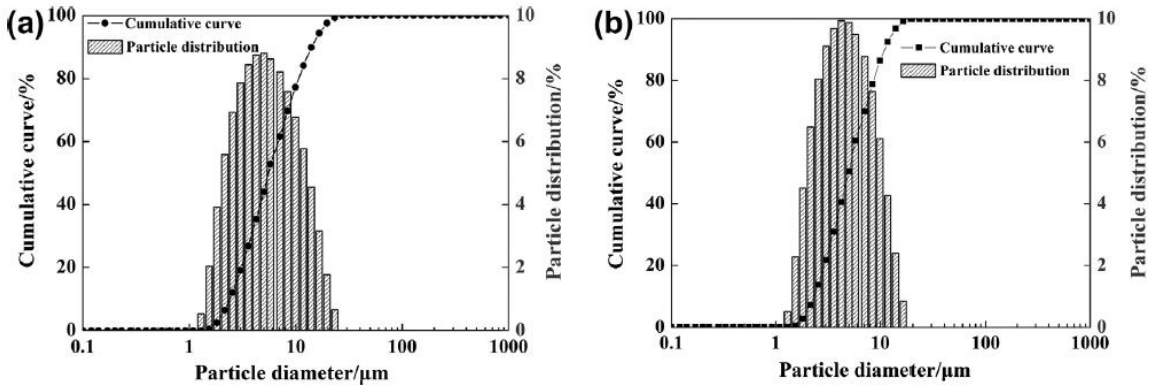

Fig. 6 - Particle size distribution, (a) mixed powder without ball mill process; (b) mixed powder after ball mill process (Ma et al., 2014)

Besides that, the powder characteristics change greatly after milling. The dispersion of the particles is greatly improved and the particles are also refined with increasing friction time. For instance, once the mixed powder is mixed for 3 hours, the spherical aggregates are broken into irregular aggregates as the mixing time continues to rise to 5 hours and 10 hours, thus, the dispersion of powder is increasing, and many individual particles appear. Figure 7 demonstrates the powder morphologies and distributions of particle sizes for these various powders with different mixing time. From the laser specific size distribution curve, it is observed that the obtained powder is trimodal and has large aggregates. The powder is gradually made unimodal after milling, and the scale of the aggregates is greatly reduced (Han et al., 2013).

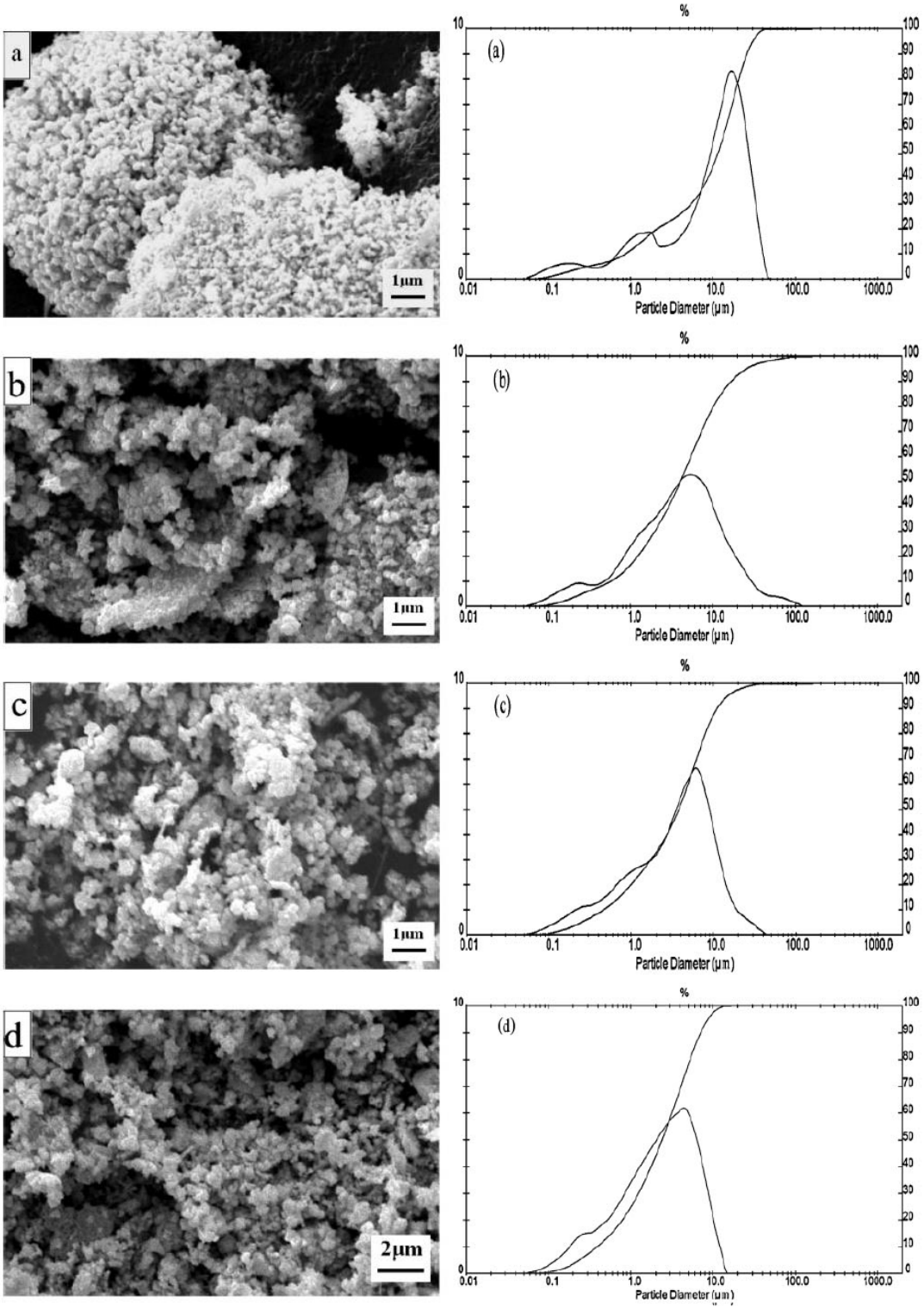

Fig. 7 - (a) as received powder; (b) powder milled for 3 h; (c) powder milled for 5 h; (d) powder milled for 10 h and particle size distribution of different powders (Han et al., 2013)

5.1 Particle Shape

The shapes of the particles are a significant factor in powder processing. The powder's properties affect both feedstock and end product. Finer powder is often used to boost sintering with a wider size range which also improves the efficiency of packing and sintering. Under the MIM process, the particle shape of the raw material powder affects the viscosity and homogeneity of the feedstock, the green parts, and the debound and sintered components. The spherical shape of the powder is important to support the packaging density of the feedstock and to enhance the mixture's flow into the mould (R. M. German, 1990). There is a certain kind of basic powder particle shapes which are the ideal shapes which mean the particles, in reality, are defective and may show features of more than one element of shape. These aspects are often in conflict. The spherical powder provides a high packing density, minimizing the amount of binder needed for moulding in addition to reducing shrinkage during sintering. However, there is no mechanical engagement at all amongst spherical particles, and the green part will have a relatively low strength specifically after the binder has been removed. On the contrary, irregular-shaped powder particles increase the viscosity of the feedstock combination, and therefore produce a lower packing density requiring more binders and result in large sintering shrinkage for the final product due to low powder loading. For the sake of better interlocking of particles, the shapes produced have high green strength and give excellent retention of the component shape during sintering (Omar & Ibrahim, 2006).

Abdul Kadir et al. investigated the implications of particle shape and size in the manufacturing of NiTi alloys by MIM on feedstock flowability and chemical content of as-sintered NiTi alloys through two diverse titanium powders. Two bunches of the powder compound consisted of Ni-Ti and Ni-TiH_2. Figure 8 indicates the SEM images of the primary Ti, TiH_2 (after ball-milled) and Ni powders used in the research. Dissimilar morphology can be noticed. Ti powder has a spherical shape with a great surface finish when TiH_2 powder is irregular and the surface structure is rough. However, the surface is rougher than Ti powder, and Ni powder is also spherical. He concluded that the rheological behaviour of spherical powder was superior to irregular powders. NiTi content was better in the overall rheological properties in terms of viscosity range, low shear sensitivity index, and activation energy rather than to Ni-TiH_2 (Abdul Kadir et al., 2018). Furthermore, micro-powder injection moulding of cemented tungsten carbide for feedstock preparation and traits has been conducted by Fayyaz et al. During MIM, they determined the powder characteristics of the initial powder in terms of particle forms that significantly impacted the viscosity and homogeneity of the feedstock, green parts, and debound and sintered parts. Figure 9 displays FESEM representations of the collected WC and WC–10Co powder. An as-collected WC contains irregularly shaped particles with a high agglomeration degree. The agglomerate clusters are cracked apart during the milling process, as indicated by the FESEM illustration of the milled power shown in Figure 9(b). Besides that, the TEM images in Figure 10 show the impact of ball milling on de-agglomeration. It expresses tremendous contrasts among as-collected and ball-milled powders. The as-collected powder is made up of strongly aggregated individual crystals while the ball-milled powder particles are mostly dispersed. In the subsequent MIM phases, any agglomeration left from the initial powder cannot be removed (A. Fayyaz et al., 2015).

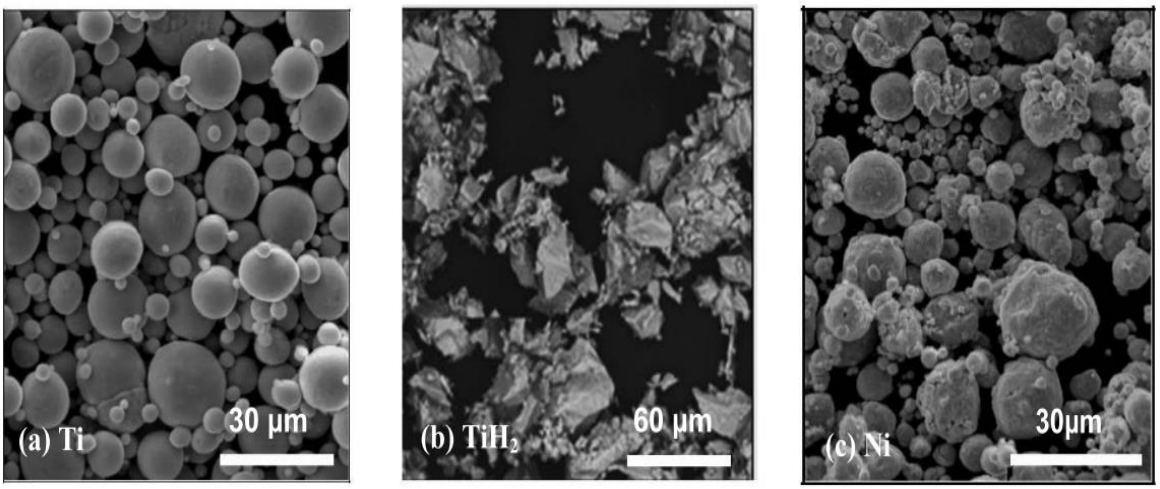

Fig. 8 - SEM of raw material primary powders: (a)Ti; (b) TiH2; (c) Ni (Abdul Kadir et al., 2018)

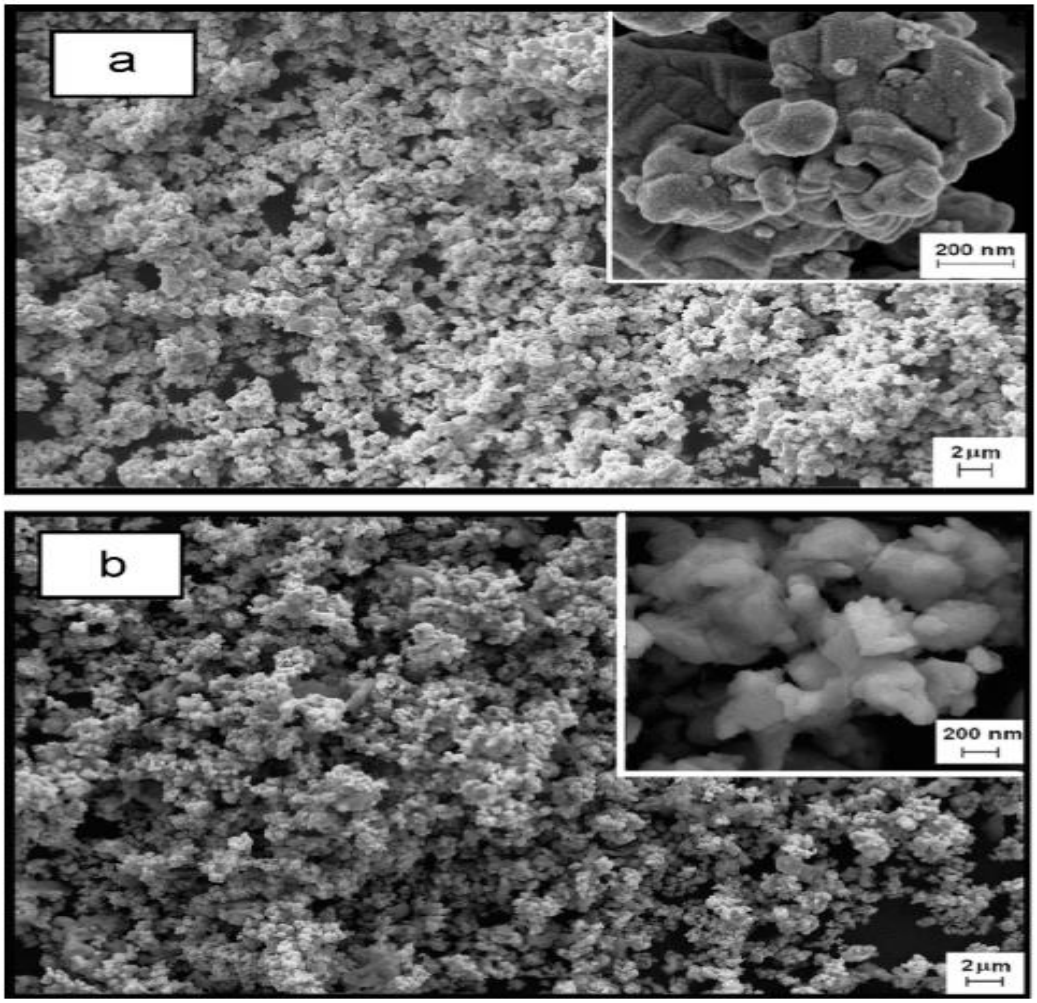

Fig. 9 - FESEM microstructure of the powders: (a) As-collected WC; (b) milled WC-10Co (A. Fayyaz et al., 2015)

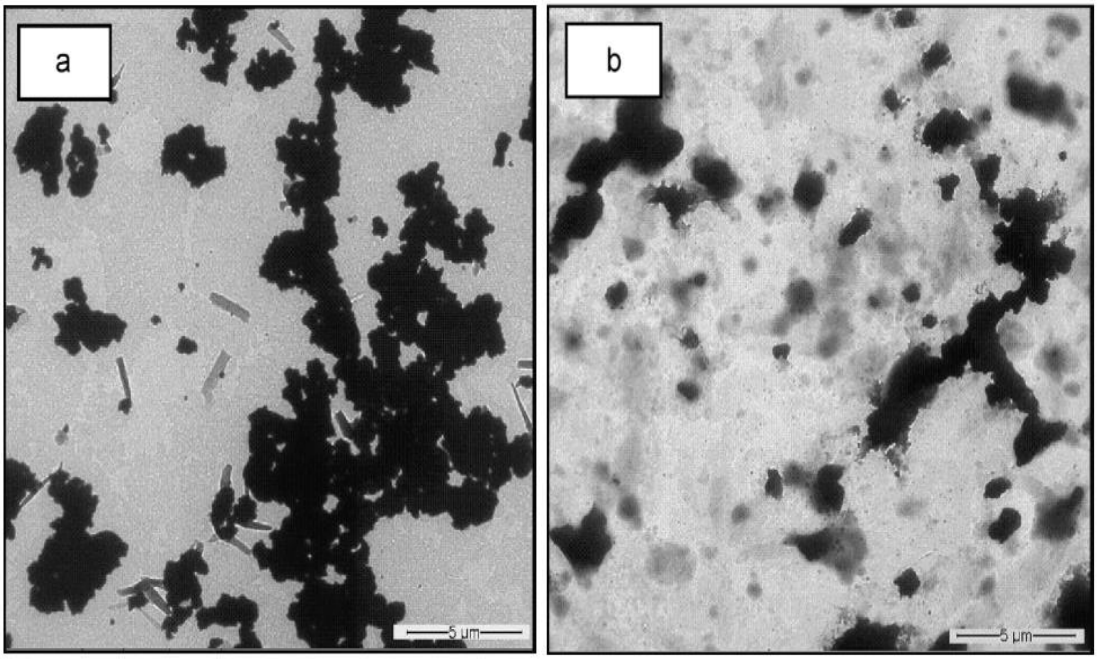

Fig. 10 - TEM microstructure of the powders: (a) As-collected WC; (b) milled WC-10Co (A. Fayyaz et al., 2015)

5.2 Particle Size Distribution

The powder and binder stipulation is noticeably more important for MIM. The particle size of powder needs to be fine enough to be manufactured with good tolerance and superiority of surface finish specifically for the manufacturing of micro- / nano-components. For the MIM method, the precondition for powder size is in the range of 4 μm and 20 μm (Gietzelt et al., 2004). Several outcomes have shown that finer powder particles result in some advantages, which are minor moulding defects, increased melting viscosity, higher sintering and shrinking rate, and finer surface finish (Randall M. German & Bose, 1997). Surprisingly, the limitations found are longer debinding time and higher costs of powder procurement. It also gives greater packing efficiency for coarser powder particle advantages in dissimilarity with finer powder, reduces sintering shrinkage rates, and shorter debinding time.

To obtain a homogenous feedstock, the particle size should increase the time, thus reducing the critical load. Strong tendency of fine powder to aggregate occurs when time increases, but a problem ordinarily turns up with fine particles, also known as agglomeration (Randall M. German & Bose, 1997), (Z. Y. Liu et al., 2003). As agglomeration occurs in the powder-binding mixture out of the initial powder remains, it causes imperfection in the sintered part, thus the mechanical characteristics of the final components are reduced. Accordingly, the de-agglomeration of powder is suggested through the MIM process to receive the appropriate physical and mechanical properties. On the other hand, the distribution slope parameter (Sw) is the parameter used to predict mobility of the feedstock. Thus, the particle size distribution on the mobility of the feedstock is also affected by the chain of the MIM process (Sotomayor et al., 2010).

$$S_w = \frac{2.56}{\log(\frac{d_{90}}{d_{10}})} \tag{4}$$

Another possible explanation for this is that when the powder exhibits a S_W of 2, there is a wide distribution, thus they are easy to mould. However, it is more complicated to mould when the value of S_W is between 4 and 5. However, when the value of S_W is greater than 7, it is the most difficult to mould.

6. Rheological Characterization of the Rheological Properties of the PIM Feedstock

There are several benefits of rheological analysis to ensure the stability of feedstock for a successful production process. Therefore, this method is a compulsory definitive rheological behaviour of the feedstock, in particular the flow behaviour index, n<1, and the reasonable value of activation energy, E. Whereas, the compact possible defects affect cracking and warping during debinding and sintering process by non-homogeneous melt flow and powder-binder segregation during injection moulding. In the end, the physical and mechanical properties of the final product are inadequate (Randall M. German & Bose, 1997). Moreover, lower mouldability index values show poor rheological properties (Abolhasani & Muhamad, 2009), and high melt viscosity has been detected as a justification for the moulding difficulty (Amin et al., 2014).

6.1 Flow behaviour index, *n*

Metal injection moulding feedstock reveals that quasi-plastic or pseudoplastic flow characteristics are successful in MIM practice. For such fluids:

$$\tau = K\dot{\gamma}^n \tag{5}$$

where τ is the shear stress, $\dot{\gamma}$ the shear rate, n the flow behaviour index, and K is a constant. The value of $n > 1$ shows a dilatant material where the metal powder and the binder are segregated at a high shear rate and smaller values (usually less than 1), indicating a higher shear sensitivity. Thus, more pseudoplasticity of the feedstock occurs, and, the better response of the viscosity to change in the shear rate is obtained (Ahn et al., 2009). As usual, viscosity (η) is the most significant rheological property for metal powder feedstock which is defined by Eq. (2). In terms of views, the viscosity is the operation of the shear rate, the temperature, the loading of the powder, the composition of the binder, and the viscosity of the binder mixture. Then, the general rate of shear-dependence of viscosity is characterized by Eq. (3) that shows the degree of shear sensitivity.

$$\eta = \frac{\tau}{\dot{\gamma}} \tag{6}$$

$$\eta = k\gamma^{n-1} \tag{7}$$

Amin et al. (2009) finalized fine particles and revealed low *n* values, and higher pseudoplastic behaviour of the feedstock. To figure the mouldability of the feedstock, the *n* value for each feedstock was calculated. In Ismail's rheological discovery by using Ni and Ti powder mixtures, the optimal range of *n* was between 0.5 and 0.7. Feedstock with a very viscous flow greater than 0.7 came from short shot defects, and deficient *n* values were caused by jetting flow contributing to binder separation. Figure 11 presents the *n* values for both feedstock. Clearly, the Ni-Ti feedstock showed better flowability compared to the Ni-TiH_2 feedstock due to the spherical shape of the Ti powder (Abdul Kadir et al., 2018).

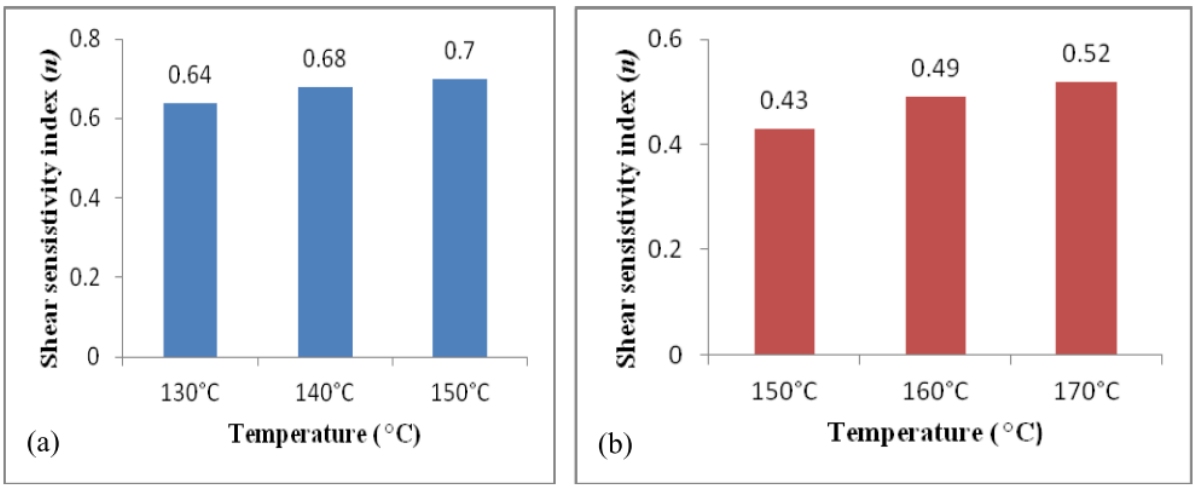

Fig. 11 - Sensitivity Index (*n*) a) Ni-Ti feedstock, b) Ni-TiH_2 feedstock (Abdul Kadir et al., 2018)

6.2 Activation Energy, *E* (Temperature Sensitivity)

Activation energy, *E*, is determined based on the Arrhenius equation by Eq. (4) where η_o is the viscosity at the reference temperature, R is the gas constant, and T is the temperature in Kelvin unit. A high value of activation energy, *E*, means high sensitivity of the viscosity to temperature and pressure, leading to the formation of defects during the injection moulding process (Ramli et al., 2011).

$$\eta = \eta_0 \exp\left(\frac{E}{RT}\right) \tag{8}$$

Temperature-dependence of the viscosity is the second key condition of the rheological characteristics of the metal injection feedstock. Subsequently, Sri et al. conducted an experiment to study the rheological properties of SS316L (MIM) feedstock set up with two sets of particle sizes which are coarse and fine powder of different powder loadings. The function of the shear rate as activation energy is demonstrated in Figure 12. The activation energy of the raw powder feedstock for the coarse powder particle corresponds with the shear rate compared to the fine powder particle, showing clearly the inversed proportion of the activation energy to the shear rate, especially at low shear levels. Moreover, in coarse powder particles, the activation energy is found to be high at higher powder loading, especially at high shear levels due to high value of flow activation energy, which demonstrates a high-temperature dependence of the feedstock on viscosity.

Consequently, everylittle fluctuation in temperature during the moulding process affects the outcome of viscosity a nd defects in the moulded components, like cracking and distortion due to stress concentration (Gille et al., 2002). The low value of activation energy affects lower temperature sensitivity, in comparison with fine powder particles, thereby reducing stress concentration, cracking, and distortion of the moulded parts (Sun et al., 2008).

Table 2 - Flow activation energy for both feedstock

Feedstock	The flow activation energy (kJ/mol)
A (Ni-Ti)	16.1
B (Ni-TiH_2)	55.72

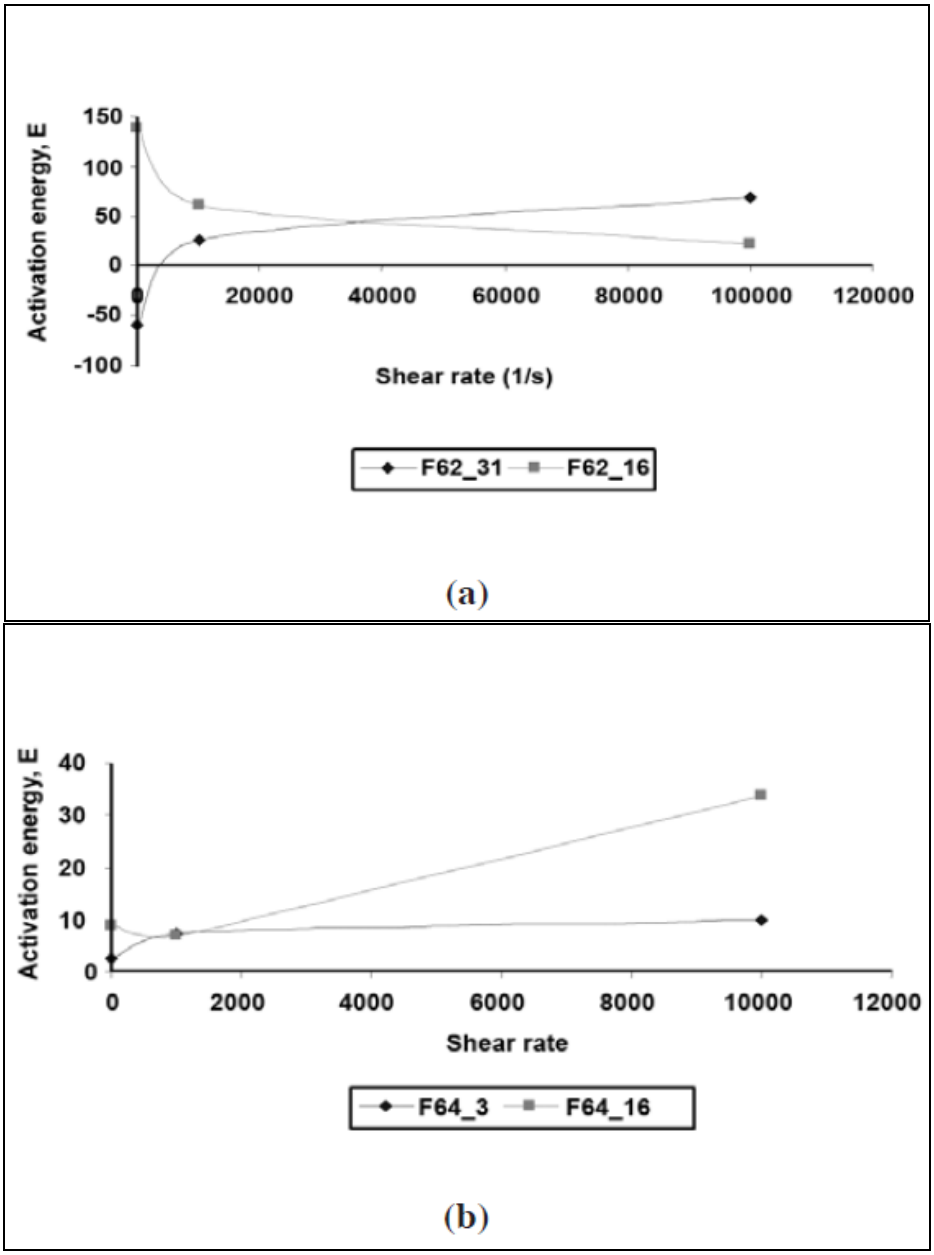

Fig. 12 - Activation energy of PIM feedstock as a function of shear rate at different powder loadings of (a) 62%; (b) 64% (Gille et al., 2002)

6.3 Mouldability index, α

The binder formulation mouldability index (α) and the MIM feedstock are measured using Eq. (5) as suggested by Weir et al. (Weir et al., 1963), where η_0 is the apparent viscosity at the reference shear rate (10 s^{-1}), γ is the apparent shear rate, n is the flow behaviour index, E_a is the flow activation energy, and R is the universal gas constant.

$$\alpha = \frac{10^9}{\eta_0} \frac{\partial \ln n / \partial \ln \gamma}{\partial \ln n / \partial (1/T)} = \frac{10^9 |n-1|}{\eta_0 \left(\frac{E_a}{R}\right)} \quad (9)$$

The higher the value, the more excellent the overall rheological properties. Figure 13 shows the general mouldability index versus solid loading. As shown in this figure, 57% of solid loading is the highest mouldability index. The three parameters ($1/\eta_{o,}1/n$, and R/E) are also plotted against the solid loading percentage. The R / E parameter sharply increases to 57 vol% followed by a decrease to 59 vol%. This could be indicated that the 57 vol% solid loading of the feedstock has the best rheological properties and is the most suitable for injection moulding (Aggarwal et al., 2006).

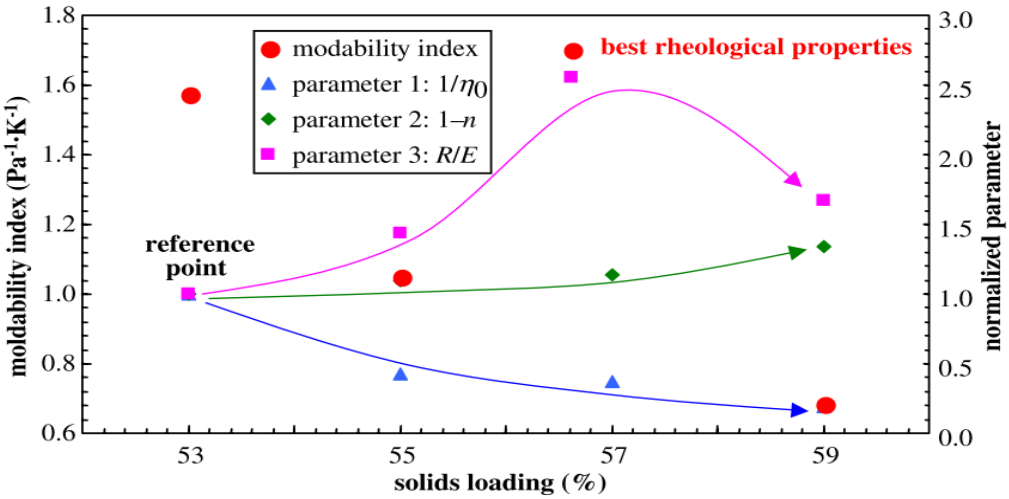

Fig. 13 - General mouldability index vs. solid loading % (Aggarwal et al., 2006)

7. Common Defects

Metal injection moulding (MIM) consists of several processing steps, and in each stage, defects can develop. The defects could result from technical factors such as poor mould design and mould production, or by the processing of related factors. The factors include incomplete kneading, insufficient moulding pressure, speed of injection, holding pressure, and non-optimized parameters for debinding and sintering. Insufficient control of the injection moulding process can result in low quality of final sections of MIM.

1. Flow mark: This is also known as flow lines. Flow marks are usually seen near the gates of the mould where the molten powder of the feedstock enters through metal injection. They do not affect the final product's quality, but are unpleasant particularly when discovered on products that should be aesthetically pleasing. The flow lines are induced by the differences in the cooling rate of the molten metal as they move through the heated barrel and mould, and solidify. Also, slow injection speed or low-pressure moulding can lead to flow mark. To overcome this problem, injection speed, mould temperature, and feedstock temperature should be increased.
2. Flash: Flash occurs when feedstock under high moulding pressure is pushed into clearances between mould components. A very high temperature or pressure of the mould during injection may also cause flash defect. Insufficient clamping force of resin-containing plates is another contributor to the flash. Thus, it is good to use lower injection speed and moulding pressure, and maximize the switch stage.
3. Residual stress: Residual stress is the stress left in the moulded part, which includes the residual stress induced by the flow and the thermally induced residual stress, which are subject to no external load after ejection (Lee et al., 2006). Only the next processing phases, which are solvent and thermal debinding, do not cause the appearance of residual stress. Due to the rapid cooling, this tension is maintained by the relative cold mould surfaces. Distortion may occur when this stress is relieved during heating at the debinding phase, either insolvent or early thermal debinding phase (Merwe & Sacks, 2013). Therefore, high temperature in the mould generally gives less residual tension rather than lower mould temperature, which adds residual stress.
4. Binder / Powder separation: The powder binder separation is also called phase segregation. The phenomenon occurs at high injection temperature and high injection pressure. Under the powder migration from the high-shear zone to the low-shear field, the binders can be separated as the feedstock moves over the narrow gate into the die cavity. It turns more extreme in the late filling stage and during the holding stage, in which the feedstock flows gradually and the strain quickly increases. Reducing the nozzle and moulding temperature decreases the separation. Therefore, optimizing the reduction of process temperature (nozzle and mould temperature) to the working limits of the feedstock can be useful to reduce powder segregation (Jenni et al., 2015).

A productive debinding process usually requires two or three phases with the same reasons the binder components are removed to ensure that the shape of the moulded compact remains flawless as before and during the debinding process. The defects emerge during an inappropriate debinding process. Table 3 shows several defects after debinding process with possible factors and cures (Fan & Hwang, 2010), (K.S.Hwang, 1996). Other than that, the benefit of the MIM process is its ability to create smooth surface finished parts with minimal surface roughness. To reach this target,

high density must be achieved and the metal surface should be exempted of sintering atmospheric reactions that prevent oxide, nitride or other reaction products from formation (J. Liu et al., 1999). There are several problem defects after the sintering process (refer to Table 4). The defects arise if sintering is improperly performed.

Table 3 - Several defects after debinding process with possible factors and cures (Hwang, 2012)**,** (Randall M. German & Animesh, 1997)

Defects	Factors	Possible cures
Cracks	• Backbone binder with low strength • Moulding pressure is too high	• Change solvent or binder type and composition • Use lower injection speed and moulding pressure
Bending/distortion	• Moulding creates residual stress	• Adjust moulding parameters
Blistering	• Inadequate removal of binders for solvent debinding • Poor distribution of binder	• Enhance solvent debinding time • Adjust binder composition
Exfoliation	• Heating rate excessively high • Wax separation to the surface	• Boost time during solvent debinding • Use slower heating rate

Table 4 - Several defect problems with possible factors and cures after sintering process (Hwang, 2012)**,** (Randall M. German & Animesh, 1997)

Defects	Factors	Possible cures
Blisters	• Rapid cooling during the sintering process	• Slow heating to allow volatile species to avoid densification before sintering
Shrinkage	• Moulding process • Powder packing	• Remove moulding flow separation and eliminate binder • Particle orientation in moulding
Pores	• Binder clusters • Gas reaction • Heating rate	• Mix binder properly to eliminate large pores • Reduce heating rate to minimize grain growth
Cracking	• Heating rate • Weld line	• Diminish the heating rate at the early stage of sintering process to increase strength • Eliminate hairline cracks at one place in the moulded part

8. Conclusion

Metal injection moulding (MIM) is a technique recently developed for the formation of metals and alloys. Besides that, this technology helps through characterization of metal powders and binder components. The grain growth inhibitor (GGI) has also been studied in relation to the starting powder and the GGI's function is to increase the values of hardness, fracture resistance, and creep resistance at certain temperatures. The present research intends to accurately formulate the flow behaviour index (n), activation energy (E), and mouldability index (α) for rheological behaviour. This study found that all MIM feedstock needs a pseudoplastic behaviour to attract the low value of flow behaviour index (n) so that the viscosity of the feedstock changes rapidly with the shear rate and displays shinning behaviour. Then, the value of low energy activation (E) should be lower to avoid any defect form after the injection process. Also, high mouldability parameter (α) is mixing great homogeneity and high stability with good feedstock characterization parameters in terms of critical powder loading, binder composition, and distribution of particle size and particle shape. This is because less defects with good mechanical properties are important to develop the final product.

9. Acknowledgement

The authors would like to thank the Ministry of Higher Education Malaysia, Universiti Teknologi MARA, for awarding research grant 600-IRMI/FRGS 5/3 (166/2019) for the financial support to conduct this research.

References

[1] Abdul Kadir, R. A., Razali, R., Mohamad Nor, N. H., Subuki, I., & Ismail, M. H. (2018). The Effect of Particles Shape and Size on Feedstock Flowibility and Chemical content of As-sintered NiTi Alloys. *IOP Conference Series: Materials Science and Engineering*, *358*(1). https://doi.org/10.1088/1757-899X/358/1/012064

[2] Abolhasani, H., & Muhamad, N. (2009). Rheological investigation of a starch-based binder and feedstock for metal injection molding. *International Journal of Mechanical and Materials Engineering*, *4*(3), 294–299.

[3] Aggarwal, G., Park, S. J., & Smid, I. (2006). Development of niobium powder injection molding: Part I. Feedstock and injection molding. *International Journal of Refractory Metals and Hard Materials*, *24*(3), 253–262. https://doi.org/10.1016/j.ijrmhm.2005.06.003

[4] Ahn, S., Park, S. J., Lee, S., Atre, S. V., & German, R. M. (2009). Effect of powders and binders on material properties and molding parameters in iron and stainless steel powder injection molding process. *Powder Technology*, *193*(2), 162–169. https://doi.org/10.1016/j.powtec.2009.03.010

[5] Al-Aqeeli, N., Saheb, N., Laoui, T., & Mohammad, K. (2014). The synthesis of nanostructured WC-based hardmetals using mechanical alloying and their direct consolidation. *Journal of Nanomaterials*, *2014*. https://doi.org/10.1155/2014/640750

[6] Amin, S. Y. M., Muhamad, N., & Jamaludin, K. R. (2014). Rheological properties analysis of WC-Co injection feedstock. *Materials Science Forum*, *773–774*(November), 880–886. https://doi.org/10.4028/www.scientific.net/MSF.773-774.880

[7] Amin, S. Y. M., Muhamad, N., Jamaludin, K. R., Fayyaza, A., & Yunn, H. S. (2012). Ball milling of WC-Co powder as injection molding feedstock. *Applied Mechanics and Materials*, *110–116*, 1425–1430. https://doi.org/10.4028/www.scientific.net/AMM.110-116.1425

[8] Baheti, V., Abbasi, R., & Militky, J. (2012). Ball milling of jute fibre wastes to prepare nanocellulose. *World Journal of Engineering*, *9*(1), 45–50. https://doi.org/10.1260/1708-5284.9.1.45

[9] Cao, M. Y., Rhee, B. O., & Chung, C. I. (1991). Usefulness of the viscosity measurement of feedstock in powder injection molding. *Advances in Powder Metallurgy*, *vol 2*, 59–73.

[10] Cao, P., & Hayat, M. D. (2020). Design strategy of binder systems and feedstock chemistry. *Feedstock Technology for Reactive Metal Injection Molding*, 43–85. https://doi.org/10.1016/b978-0-12-817501-9.00002-8

[11] Chen, L., & Al, F. (2001). *Mechanical Alloying- Parameters* (Vol. 18, Issue 6).

[12] Chen, Y., Yang, Y., Yang, G., Wang, L., & Wu, M. (2018). Fabrication of WC-TiC-Co Cemented Carbide at Different Heating Rate by Micro-FAST process. *MATEC Web of Conferences*, *190*, 0–3. https://doi.org/10.1051/matecconf/201819010006

[13] Childs, T. (2000). Metal Machining. *Metal Machining*. https://doi.org/10.1016/c2009-0-23990-0

[14] El-Eskandarany, M. S. (2015). Controlling the powder milling process. In *Mechanical Alloying*. https://doi.org/10.1016/b978-1-4557-7752-5.00003-6

[15] Fabijanić, T. A., Alar, Ž., & Ćorić, D. (2016). Influence of consolidation process and sintering temperature on microstructure and mechanical properties of near nano- and nano-structured WC-Co cemented carbides. *International Journal of Refractory Metals and Hard Materials*, *54*, 82–89. https://doi.org/10.1016/j.ijrmhm.2015.07.017

[16] Fabijanić, T. A., Alar, Ž., & Pötschke, J. (2014). Potentials of nanostructured WC-Co hardmetal as reference material for Vickers hardness. *International Journal of Refractory Metals and Hard Materials*, *50*, 126–132. https://doi.org/10.1016/j.ijrmhm.2014.12.006

[17] Fan, Y. L., & Hwang, K. . (2010). Defect formation and its relevance to binder content and binder redistribution during thermal debinding of PIM compacts. *Proceedings of the 2010 PM World Congress, EPMA, Shrewsbury*, *4*, 595–601.

[18] Fayyaz, A., Muhamad, N., Sulong, A. ., Yunn, H. ., Amin, S. Y. ., & Rajabi, J. (2015). Micro-powder injection molding of cemented tungsten carbide: Feedstock preparation and properties. *Ceramics International*, *41*(3), 3605–3612. https://doi.org/10.1016/j.ceramint.2014.11.022

[19] Fayyaz, Abdolali, Muhamad, N., Sulong, A. B., Rajabi, J., & Wong, Y. N. (2014). Fabrication of cemented tungsten carbide components by micro-powder injection moulding. *Journal of Materials Processing Technology*, *214*(7), 1436–1444. https://doi.org/10.1016/j.jmatprotec.2014.02.006

[20] German, R. M. (1990). *Powder injection molding*. Metal Powder Industries Federation.

[21] German, Randall M., & Animesh, B. (1997). *Injection Moulding of Metal and Ceramics*.

[22] German, Randall M., & Bose, A. (1997). *Injection moulding of metals and ceramics*.

[23] Gietzelt, T., Jacobi, O., Piotter, V., Ruprecht, R., & Hausselt, J. (2004). Development of a micro annular gear pump by micro powder injection molding. *Journal of Materials Science*, *39*(6), 2113–2119. https://doi.org/10.1023/B:JMSC.0000017774.64153.d9

[24] Gille, G., Szesny, B., Dreyer, K., Van Den Berg, H., Schmidt, J., Gestrich, T., & Leitner, G. (2002). *Submicron and ultrafine grained hardmetals for microdrills and metal cutting inserts*. *20*, 3–22.

[25] Han, Y., Fan, J. L., Liu, T., Cheng, H. C., Gao, Y., & Tian, J. M. (2013). Influence of ball milling on powder characteristics and feedstock rheological behaviours of injection moulded ultrafine 98W-1Ni-1Fe. *Powder*

Metallurgy, *56*(2), 135–142. https://doi.org/10.1179/1743290112Y.0000000028

[26] Hwang, K. S. (2012). Common defects in metal injection molding (MIM). In *Handbook of Metal Injection Molding* (Issue Mim). Woodhead Publishing Limited. https://doi.org/10.1533/9780857096234.2.235

[27] Jenni, M., Schimmer, L., Zauner, R., Stampfl, J., & Morris, J. (2015). *Quantitative study of powder binder separation of feedstocks*. *January 2008*.

[28] Jiang, A., Wen, B., & Li, Q. (2015). *Fabrication of WC-TiC-6%Co Hard Metals by micro-powder injection moulding*. *Iwmecs*, 543–547. https://doi.org/10.2991/iwmecs-15.2015.107

[29] K.S.Hwang. (1996). Fundamentals of debinding processes in powder injection molding. *Reviews in Particulate Materials*, *4*(71–103).

[30] Karatas, C., Kocer, A., Ünal, H. I., & Saritas, S. (2004). Rheological properties of feedstocks prepared with steatite powder and polyethylene-based thermoplastic binder. *Journal of Materials Processing Technology*, *152*(1), 77–83. https://doi.org/10.1016/j.jmatprotec.2004.03.009

[31] Lee, K. H., Cha, S. I., Kim, B. K., & Hong, S. H. (2006). Effect of WC/TiC grain size ratio on microstructure and mechanical properties of WC-TiC-Co cemented carbides. *International Journal of Refractory Metals and Hard Materials*. https://doi.org/10.1016/j.ijrmhm.2005.04.018

[32] Li, Y., Li, L., & Khalil, K. A. (2007). Effect of powder loading on metal injection molding stainless steels. *Journal of Materials Processing Technology*, *183*(2–3), 432–439. https://doi.org/10.1016/j.jmatprotec.2006.10.039

[33] Liu, J., Lal, A., & German, R. M. (1999). Densification and shape retention in supersolidus liquid phase sintering. *Acta Materialia*, *47*(4615–4626).

[34] Liu, Z. Y., Loh, N. H., & Tor, S. B. (2001). Binder system for micropowder injection molding. *Materials Letters*, *48*(1), 31–38. https://doi.org/10.1016/S0167-577X(00)00276-7

[35] Liu, Z. Y., Loh, N. H., Tor, S. B., & Khor, K. A. (2003). Characterization of powder injection molding feedstock. *Materials Characterization*, *49*(4), 313–320. https://doi.org/10.1016/S1044-5803(02)00282-6

[36] M. Y. Anwar and H. Davies. (1995). A novel binder system for powder injection molding. *Adv. Powder Metall. Part. Mater.*, *2*, 6.

[37] Ma, J., Qin, M., Zhang, L., Tian, L., Li, R., Chen, P., & Qu, X. (2014). Effect of ball milling on the rheology and particle characteristics of Fe-50%Ni powder injection molding feedstock. *Journal of Alloys and Compounds*, *590*, 41–45. https://doi.org/10.1016/j.jallcom.2013.12.080

[38] Magdalinovic, N., Trumic, M., Trumic, M., & Andric, L. (2012). The optimal ball diameter in a mill. *Physicochemical Problems of Mineral Processing*, *48*(2), 329–339. https://doi.org/10.5277/ppmp120201

[39] Mahmoodan, M., Aliakbarzadeh, H., & Gholamipour, R. (2009). Int . Journal of Refractory Metals & Hard Materials Microstructural and mechanical characterization of high energy ball milled and sintered WC – 10 wt % Co – x TaC nano powders. *International Journal of Refractory Metals and Hard Materials*, *27*(4), 801–805. https://doi.org/10.1016/j.ijrmhm.2009.02.001

[40] Mannesson, K. (n.d.). *WC Grain Growth during Sintering of Cemented Carbides*. KTH Industrial Engineering and Management, Stockholm, Sweden.

[41] Merwe, R. Van Der, & Sacks, N. (2013). Int . Journal of Refractory Metals and Hard Materials Effect of TaC and TiC on the friction and dry sliding wear of WC – 6 wt .% Co cemented carbides against steel counterfaces. *RMHM*, *41*, 94–102. https://doi.org/10.1016/j.ijrmhm.2013.02.009

[42] Morton, C. W., Wills, D. J., & Stjernberg, K. (2005). The temperature ranges for maximum effectiveness of grain growth inhibitors in WC–Co alloys. *International Journal of Refractory Metals and Hard Materials*, *23*(4–6), 287–293. https://doi.org/10.1016/j.ijrmhm.2005.05.011

[43] Omar, M. A., & Ibrahim, R. (2006). Metal Injection Moulding : an Advanced Processing Technology. *Journal of Industrial Technology*, *15*(1), 11–22.

[44] Pahroraji, H. F., Irwan Ibrahim, M. H., Muniandy, P., Amin, S. Y. M., & Alias, S. K. (2020). Parameter optimization of WC-TaC-6Co green part in injection moulding using taguchi method. *IOP Conference Series: Materials Science and Engineering*, *834*(1). https://doi.org/10.1088/1757-899X/834/1/012077

[45] Prathabrao, M., Amin, S. Y. M., & Ibrahim, M. H. I. (2017). Review on Sintering Process of WC-Co Cemented Carbide in Metal Injection Molding Technology. *IOP Conference Series: Materials Science and Engineering*, *165*(1). https://doi.org/10.1088/1757-899X/165/1/012017

[46] Quinard, C., Barriere, T., & Gelin, J. C. (2009). Development and property identification of 316L stainless steel feedstock for PIM and μPIM. *Powder Technology*, *190*(1–2), 123–128. https://doi.org/10.1016/j.powtec.2008.04.044

[47] Ramli, M. I., Sulong, A. B., Arifin, A., Muchtar, A., & Muhamad, N. (2011). Powder Injection Molding of SS316L/HA Composite: Rheological Properties and Mechanical Properties of the Green Part Mohd. *Key Engineering Materials*, *471–472*(February), 409–414. https://doi.org/10.4028/www.scientific.net/KEM.471-472.409

[48] Siwak, P., & Garbiec, D. (2016). Microstructure and mechanical properties of WC − Co , WC − Co − Cr 3 C 2 and WC − Co − TaC cermets fabricated by spark plasma sintering. *Transactions of Nonferrous Metals Society of*

China, *26*(10), 2641–2646. https://doi.org/10.1016/S1003-6326(16)64390-X

[49] Sotomayor, M. E., Varez, A., & Levenfeld, B. (2010). Influence of powder size distribution on rheological properties of 316L powder injection moulding feedstocks. *Powder Technology*, *200*(November 2015), 30–36. https://doi.org/10.1016/j.powtec.2010.02.003

[50] SU, W., SUN, Y., YANG, H., ZHANG, X., & RUAN, J. (2015). Effects of TaC on microstructure and mechanical properties of coarse grained WC–9Co cemented carbides. *Transactions of Nonferrous Metals Society of China*, *25*(4), 1194–1199. https://doi.org/10.1016/S1003-6326(15)63715-3

[51] Subaşı, M., Safarian, A., & Karataş, Ç. (2019). *An investigation on characteristics and rheological behaviour of titanium injection moulding feedstocks with thermoplastic-based binders*. *5899*. https://doi.org/10.1080/00325899.2019.1635305

[52] Sun, L., Jia, C., Cao, R., & Lin, C. (2008). *Effects of Cr 3 C 2 additions on the densification , grain growth and properties of ultrafine WC – 11Co composites by spark plasma sintering*. *26*, 357–361. https://doi.org/10.1016/j.ijrmhm.2007.08.009

[53] Thornagel, M. (2010). Simulating flow can help avoid mould mistakes. *Metal Powder Report*, *65*(3), 26–29. https://doi.org/10.1016/S0026-0657(10)70072-2

[54] Weidow, J., Norgren, S., & Andrén, H. (2009). Effect of V , Cr and Mn additions on the microstructure of WC – Co. *International Journal of Refractory Metals and Hard Materials*, *27*(5), 817–822. https://doi.org/10.1016/j.ijrmhm.2009.02.002

[55] Weir, F. E., Doyle, M. E., & Norton, D. G. (1963). Moldability of plastics based on melt rheology. *SPE Trans*, *3*, 32–336.

[56] Zakaria, H., Muhamad, N., Sulong, A. B., Irwan Ibrahim, M. H., & Foudzi, F. (2014). Moldability characteristics of 3 mol% yttria stabilized zirconia feedstock for micro-powder injection molding process. *Sains Malaysiana*, *43*(1), 129–136.

[57] Zhang, F. L., Zhu, M., & Wang, C. Y. (2008). Parameters optimization in the planetary ball milling of nanostructured tungsten carbide/cobalt powder. *International Journal of Refractory Metals and Hard Materials*, *26*(4), 329–333. https://doi.org/10.1016/j.ijrmhm.2007.08.005